JOURNAL OF OPTOELECTRONICS AND ADVANCED MATERIALS Vol. 10, No. 10, October 2008, p. 2592 - 2598

Polycrystalline indium-doped ZnO thin films: preparation and characterization

S. ILICAN*, Y. CAGLAR, M. CAGLAR, B. DEMIRCI
Department of Physics, Anadolu University, Eskisehir, 26470, Turkey

Zinc oxide (ZnO) and indium-doped zinc oxide (IZO) thin films have been deposited onto glass substrates by the spray pyrolysis method. The variations of the structural, electrical and optical properties with the indium incorporation were investigated. The crystal structure and orientation of the ZnO and IZO thin films were investigated by XRD patterns. All the deposited films are polycrystalline in nature. The grain sizes were calculated almost 31-36 nm. Morphological characterization and compositions of the films were performed by SEM and EDX analyses, respectively. It was observed that the surface morphologies of the films are almost uniform particle size distribution for the films. The optical absorbance through the films was measured spectrophotometrically in the wavelength range 200–900 nm. The optical band gap, Urbach parameters and optical parameters were determined. The electrical resistivity was obtained by the Van der Pauw method in dark and under UV-illumination. The effect of the light on the films shows that the obtained thin films can be used as a photovoltaic material.

(Received March 17, 2008; accepted August 14, 2008)

Keywords: Indium-doped ZnO, Spray pyrolysis, Van der Pauw method, Optical band gap, X-ray diffraction.

1. Introduction

Transparent conductive oxide (TCO) films are great of importance due to their applications in various electronic and optoelectronic devices, such as solar cells, gas sensors, varistors and diodes [1-6]. Among them ZnO is the most attractive material because of low toxicity, a wide band gap material (~3.3 eV; at room temperature) and its many applications due to its good electrical and optical properties. In order to improve these properties can be doped with some elements [7-10]. Especially, Group III elements such as In^{3+}, Al^{3+}, Ga^{3+} are used to improve and/or control the electrical conductivity. These dopants act as a donor when it occupies a substitutional position for Zn^{2+} cation or an interstitial position in the ZnO lattice. The efficiency of the dopant element related to its electronegativity and the ionic radius.

In-doped ZnO films have been deposited different methods such as sputtering, electrodeposition process, sol-gel deposition and spray pyrolysis [11-16]. In this study, the films have been deposited by spray pyrolysis method. This method has variety advantages such as the low-cost, no-vacuum and easy doping.

There have been extensive studies on the crystalline structure and optical transmittance of In-doped ZnO thin films prepared by spray pyrolysis method [15, 17-19]. However, there are few studies on the optical constants of In-doped ZnO thin films.

In our previous works we reported on ZnO and indium doped ZnO films prepared by spray pyrohisis [20-22].

In this work, we report the effect of indium incorporation on the structural, morphological, optical and electrical properties of the sprayed ZnO thin films.

2. Experimental

ZnO and IZO thin films were deposited onto glass substrates using the spray pyrolysis method at 450 ^{o}C substrate temperature. 0.2 M solution of $Zn(CH_3COO)_2.2H_2O$ diluted in methanol and deionized water (3:1) was used for all the films. For indium doping, $InCl_3$ was added to starting solution. The In/Zn ratio in the solution was 0 %, 1 %, 3 %, and 5 % (These films were named as ZnO, IZO1, IZO3 and IZO5, respectively). The details of spray pyrolysis set-up are given in elsewhere [14]. Nitrogen was used as the carrier gas (p_N= 0.2 bar). During deposition, solution flow-rate was held constant at 4 mlmin^{-1}, and the ultrasonic nozzle to substrate distance was 30 cm. The thicknesses of the films were measured by weight-difference method using a sensitive semi-microbalance. The film thicknesses were found to be approximately 600 nm.

The crystal structure of the films was analyzed with RIGAKU RINT 2200 Series X-Ray Automatic Diffractometer with CuK_α (λ=1.54059 Å) radiation, at room temperature. The value of 2θ was swapped between 20º and 60º. Surface morphology was studied using ZEISS EVO-50 model SEM. The absorption spectra of the films were recorded from 200 nm to 900 nm wavelength using SHIMADZU UV-2450 UV–VIS spectrophotometer. The films were found to be n-type by using hot-probe method. The electrical measurements were carried out using the four-probe Van der Pauw configuration and silver paste for the contacts in dark and under a light which has wavelength of 254 nm. These films were illuminated by a 100W UV-lamp.

3. Results and Discussion

3.1. Crystal structure and morphological properties of ZnO and IZO thin films

The crystal structure of the ZnO and IZO thin films were investigated by X-ray diffraction (XRD) patterns.

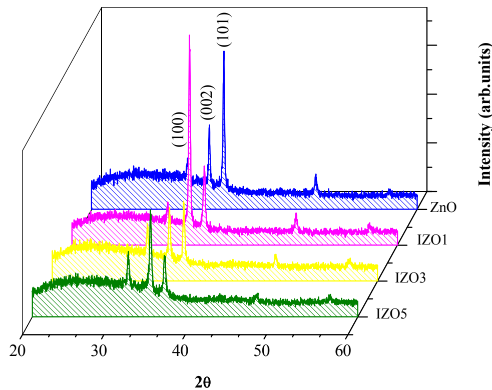

Fig. 1. X-ray diffraction spectra of undoped ZnO and IZO thin films.

Fig. 1 shows the diffraction patterns of the films. As seen in this figure, the films are polycrystalline with hexagonal wurtzite type structure. The crystallinity of ZnO films decreases when the indium doping concentration increases. As shown in Fig. 1, ZnO and IZO3 thin film have (101) as the preferred orientation, and IZO1 and IZO5 thin film have (002) as the preferred orientation.

Table 1. Elemental weights (wt.%) of Zn, O and In elements in the thin films.

	Zinc (wt.%)	Oxygen (wt.%)	Indium (wt.%)
ZnO	34.87	65.13	---
IZO1	33.13	65.75	1.12
IZO3	38.42	58.06	3.52
IZO5	33.07	61.80	5.14

For the films 2θ and *d-values* are given in Table 1. The lattice parameter of *a* and *c* calculated using eq. (1) for the films [20].

$$\frac{1}{d^2} = \frac{4}{3}\left(\frac{h^2 + hk + k^2}{a^2}\right) + \frac{l^2}{c^2} \tag{1}$$

These values are presented in Fig. 2.

The grain size of crystallites was calculated using a well-known Scherrer's formula [20]. The grain size values are given found to be 35.80 nm, 35.62 nm, 31.30 nm and 30.90 nm for IZO, IZO1, IZO3 and IZO5, respectively. It can be seen that as long as the indium content increases the grain size of the films decreases.

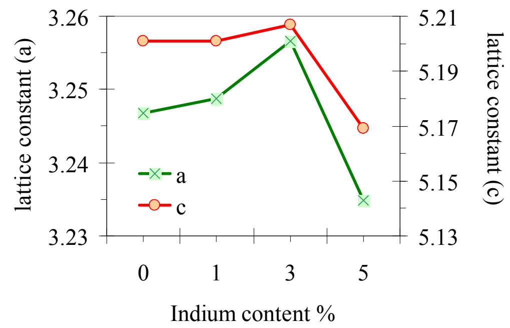

Fig. 2. Variety of lattice constants with indium content.

The texture coefficient *TC(hkl)* have been also calculated from the x-ray data using the well-known formula [21]

$$TC(hkl) = \frac{I(hkl)/I_o(hkl)}{N^{-1}\sum_n I(hkl)/I_o(hkl)} \tag{2}$$

where *I(hkl)* is the measured relative intensity of a plane *(hkl)*, $I_o(hkl)$ is the standard intensity of the plane *(hkl)* taken from the JCPDS data, *N* is the reflection number and *n* is the number of diffraction peaks. *TC(hkl)* values for major three peaks of the thin films are presented in Fig. 3.

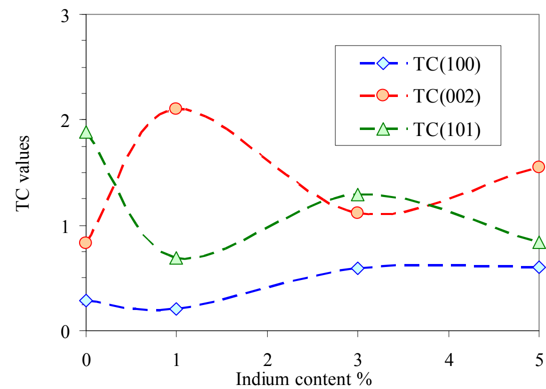

Fig. 3. Variation of TC(hkl) values with indium content

It was observed that in 1% In-doped ZnO thin film the (002) peak was having the highest texture coefficient.

Fig. 4 show scanning electron micrographs (SEM) of the ZnO and IZO thin film at 50000 and 100000 magnifications. It was seen that the surface morphologies of ZnO films were almost homogeneous. It can be noticed that the microstructure of the films is influenced by the introduction of indium atoms as dopant. For undoped ZnO thin film, the film is composed of regular and round grains with approximately 50 nm average diameter. Depending on the increasing indium concentration, the surface morphologies of the films were changed. These SEM micrographs show different morphologies of the surface grains, which depend on indium concentration.

The EDX spectra of the films are shown in Fig. 5.

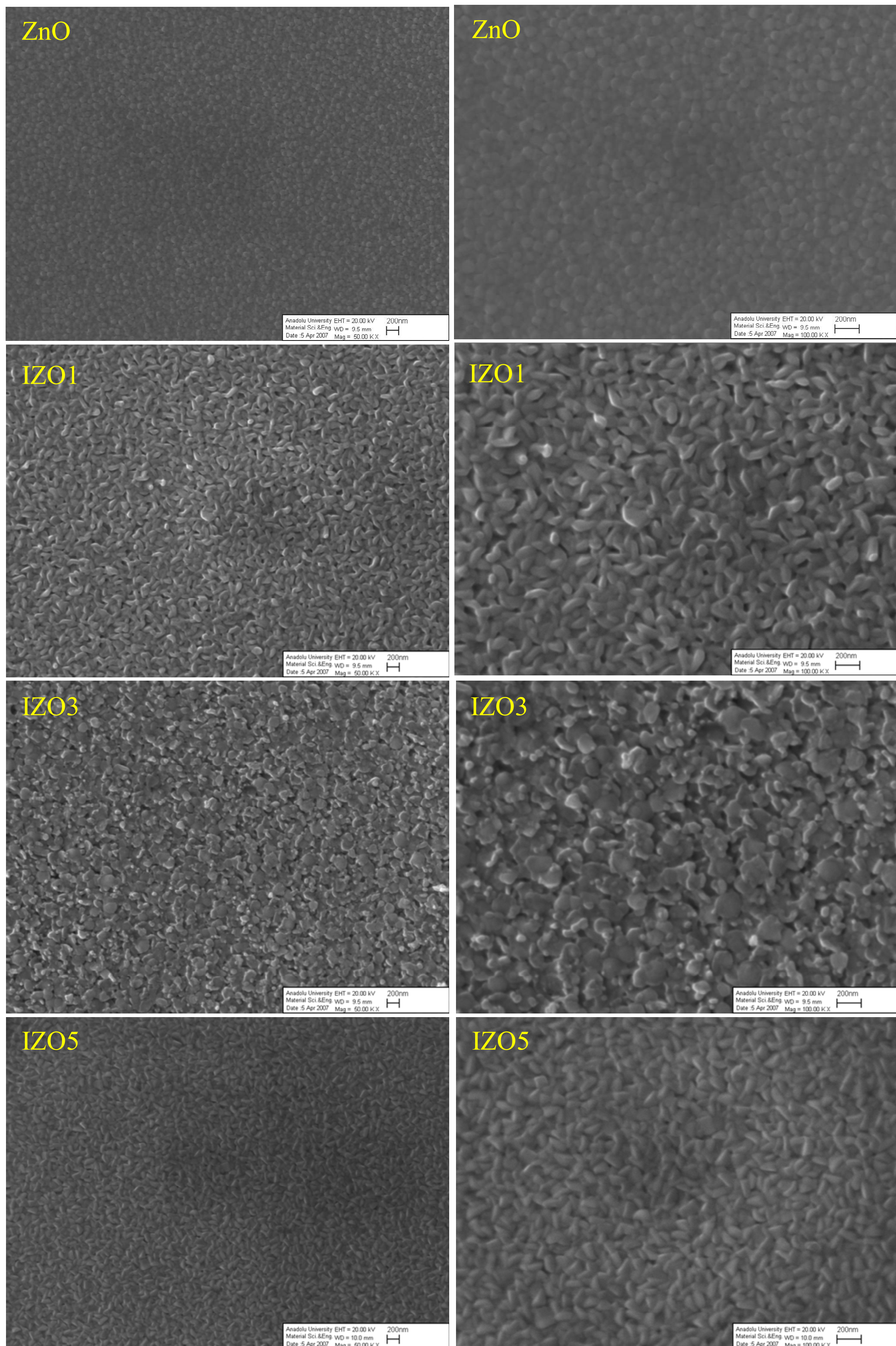

Fig. 4. SEM images of ZnO and IZO thin films (50000 magnifications on the left sides, 100000 magnifications on the right).

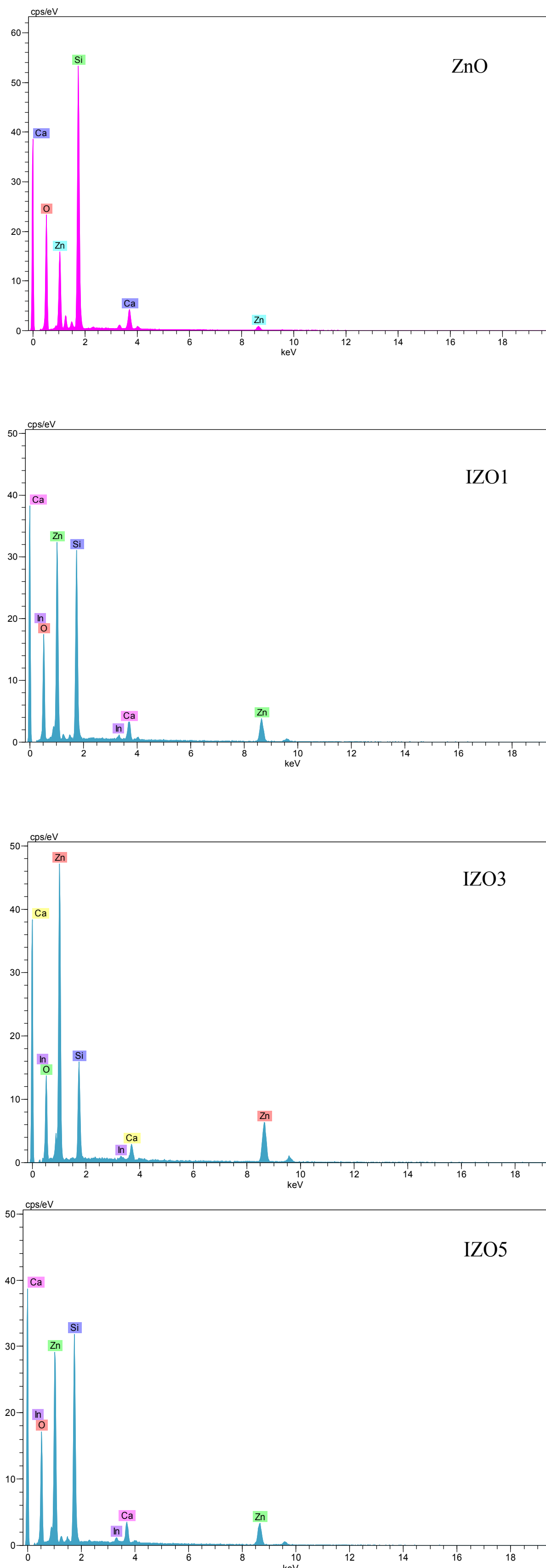

Fig. 5. EDX spectra of the films.

EDX analyses show that Zn, O and In elements in the starting solution present in the solid film. The Si and Ca elements that are not expected to be in solid films may probably result from the glass substrates. Elemental weights (wt.%) of Zn, O and In elements in the ZnO and IZO thin films are listed in Table 1. These spectra show that the expected elements exist in the solid films.

3.2. Optical properties of ZnO and IZO thin films

The optical transmittance spectra of ZnO and IZO thin films are shown in Fig. 6.

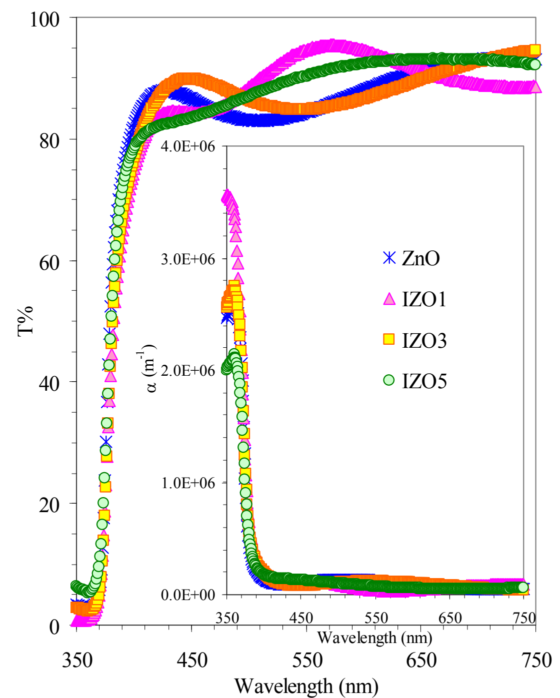

Fig. 6. Transmittance and absorption coefficient spectra of all the films.

The average transmittance value of the thin films are >88% in the visible range. Inset graph of the Fig. 6 shows the absorption coefficient spectra of the films. The direct band gaps of the films are determined by optical method by using absorption values. The optical band gap of the films is determined by the following relationship [25]

$$(\alpha h\nu) = B(h\nu - E_g)^{1/2} \quad (3)$$

where B is an energy-independent constant between 10^7 and 10^8 m^{-1} and E_g is the optical band gap. The values of the direct optical band gap E_g values were obtained from the intercept of $(\alpha h\nu)^2$ versus $h\nu$ curves plotted. Determined E_g values are given in Fig. 7.

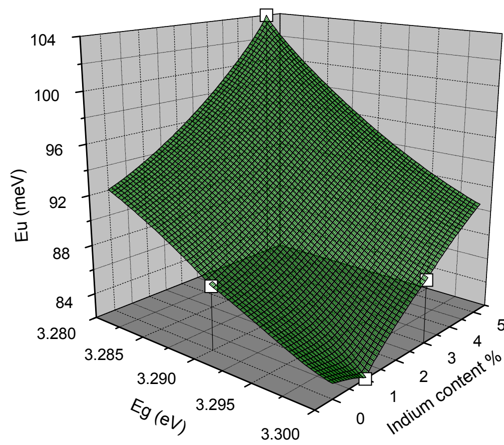

Fig. 7. Variety of optical band gaps and Urbach energies of the thin films with indium content.

B constants are found to be between 2.20x10^7 and 3.27×10^7 m^{-1}. Increase in the E_g values could be attributed to the indium atoms incorporated into the ZnO lattice. The widening of the E_g is generally attributed to the Burstein-Moss shift. On the other hand, it was seen that the higher indium content (for %In>3) caused to decrease in the E_g values. The trend of decreasing on the E_g may be attributed to the band shrinkage effect because of increasing carrier concentration.

The absorption coefficient near the band edge shows an exponential dependence on photon energy [26]

$$\alpha = \alpha_o \exp\left[\frac{h\nu - E_I}{E_U}\right] \tag{4}$$

where E_U is the Urbach energy which corresponds to the width of the band tail, E_I and α_o are constant.

Thus, a plot of $ln\alpha$ vs. $h\nu$ should be linear and Urbach energy can be obtained from the slope. The calculated values are given in Fig. 7. Urbach energy values of the films decrease with increasing indium content. The indium content is responsible for the width of localized states in the optical band of the films.

3.3. Optical constants of ZnO and IZO thin films

The complex optical refractive index of the films is describes by the following relation [27],

$$\hat{n} = n(\omega) + ik(\omega) \tag{5}$$

where n is the real part and k is the imaginary part (extinction coefficient) of complex refractive index. The refractive index of the films was determined from the following relation [28],

$$n = \left(\frac{1+R}{1-R}\right) + \sqrt{\frac{4R}{(1-R)^2} - k^2} \tag{6}$$

The n and k values decrease up to certain value with increasing wavelength and these values changes with the indium dopant (Table 2).

The dielectric constant is defined as, $\varepsilon(\omega)=\varepsilon_1(\omega)+i\varepsilon_2(\omega)$ and real and imaginary parts of the dielectric constant are related to the n and k values. The ε_1 and ε_2 values were calculated using the formulas [29],

$$\varepsilon_1(\omega) = n^2(\omega) - k^2(\omega) \tag{7}$$

$$\varepsilon_2(\omega) = 2n(\omega)k(\omega) \tag{8}$$

Both ε_1 and ε_2 values decrease with increasing wavelength. These values were calculated at 400 nm (Table 2).

Table 2. Optical constants of the ZnO and IZO thin films (at λ=400nm).

	n	$kx10^{-4}$	ε_1	$\varepsilon_2 x10^{-2}$
ZnO	1.6119	46	2.5983	1.49
IZO1	1.7956	68	3.2240	2.46
IZO3	1.7492	63	3.0597	2.21
IZO5	1.7031	57	2.9005	1.93

The optical constants of ZnO film initial increase with incorporation indium dopant element, and then, as indium dopant is increasing these values decrease.

3.4. Electrical conductivity of ZnO and IZO thin films

Hot probe method was used in order to determine conductivity type. It was seen that all the films exhibit n-type conductivity, which is attributed to a deviation from stoichiometry, due to the oxygen vacancies and interstitial zinc and/or indium atoms. Both vacancies and interstitial atoms act as donors.

The electrical resistivity values of ZnO and IZO films in dark and under UV-illumination were calculated by using Van der Pauw method [30]. The electrical resistivity of ZnO films as a function of indium content are plotted in Fig. 8.

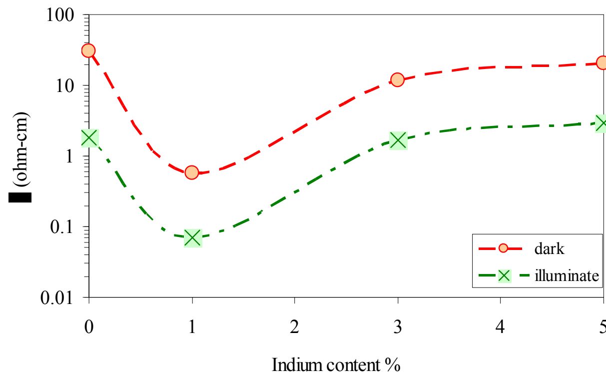

Fig. 8. The electrical resistivity of ZnO films as a function of indium content.

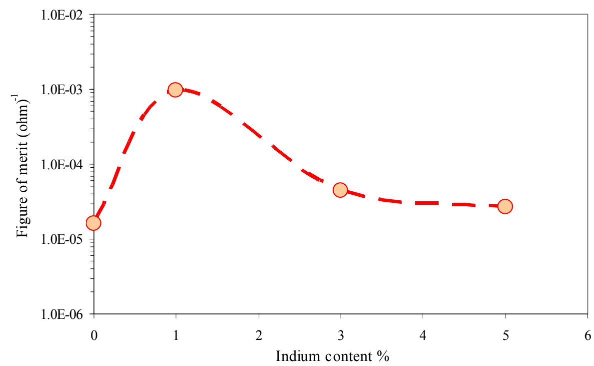

Fig. 9. Figure of merit of the thin films.

It is shown that indium content is a parameter affects the electrical properties of these films. It is seen that as indium is incorporated to the ZnO films, the electrical resistivity first decreases and then increases. The lowest resistivity value was obtained for the films doped with 1% of In. An initial decrease in the resistivity is due to an increase in the free-electron concentration with indium incorporation in the ZnO film. In the other words, it can be attributed to the optimal incorporation of indium atoms into the lattice, increasing the donor concentration and contributing to a decrease of the resistivity. The adding more indium in the ZnO film, the high indium concentration will also increase the scattering process and therefore the majority carrier mobility is decreased. It is also observed that electrical resistivity of these films decreased when exposed to UV-illumination. This indicates that the UV-illumination increases the production of electron-hole pairs. So, the obtained ZnO thin films can be used as a photovoltaic material.

3.5. Figure of merit of ZnO and IZO thin films

The films must have a low resistivity and a low absorption coefficient in the visible region for application on optoelectronic devices. To determine a film whether or not has these properties, the figure of merit (*FOM*) is calculated by using following equation [31]

$$FOM = \frac{1}{\alpha\rho} \tag{9}$$

The variation of the calculated *FOM* values of the thin films with indium content is shown in Fig. 9. It is seen that the largest value was obtained for films doped with 1 % of In.

4. Conclusions

Undoped and In-doped ZnO thin films were deposited by the spray pyrolysis method at 450 ^{o}C substrate temperature. The effects of indium doping on the structural, morphological, optical and electrical properties of ZnO and IZO thin films were investigated. All the deposited films are polycrystalline in nature. The SEM images of the thin films showed that the surface morphology is affected by the indium content. All the films have high transparency. The Burstein-Moss effect was observed the indium incorporation to ZnO thin film (for %In$\leq$3). But, it was seen that the higher indium content (for %In>3) caused to the band shrinkage effect. ZnO thin film doped with 1% indium, presents the low resistivity 5.63×10^{-1} Ωcm associated to a high transmittance ~90%. This film has characteristics required for application on optoelectronic devices, because of the highest *FOM* value. When this film was illuminated by the UV lamp, its resistivity value decreased to 7.09×10^{-2} Ωcm. So, especially 1% In-doped ZnO thin film is good TCO material and suitable for the solar cell applications.

References

[1] M. Berginski, J. Hüpkes, W. Reetz, B. Rech, M. Wuttig, Thin Solid Films, in press (2007).
[2] W. J. Jeong, S. K. Kim, G. C. Park, Thin Solid Films 506– 507 180 (2006).
[3] M. Suchea, S. Christoulakis, K. Moschovis, N. Katsarakis, G. Kiriakidis, Thin Solid Films **515** 551 (2006).
[4] Anna Og. Dikovska, Petar A. Atanasov, Svetlen Tonchev, Joao Ferreira, Ludovic Escoubas, Sensors and Actuators A **140** 19 (2007).
[5] E. Suvaci, I. O. Ozer, Journal of the European Ceramic Society **25** 1663 (2005).
[6] E. Gur, S. Tuzemen, B. Kilic, C. Coskun, C. J. Phys. Cond. Matter. **19** 196206 (2007).

[7] M. Miki-Yoshida, F. Paraguay-Delgado, W. Estrada-Lopez, E. Andrade, Thin Solid Films **376** 99 (2000).
[8] S. Ilican, Y. Caglar, M. Caglar, F. Yakuphanoglu, Physica E **35** 131 (2006).
[9] F. Yakuphanoglu, Y. Caglar, S. Ilican, M. Caglar, Physica B **394** 86 (2007).
[10] M. Caglar, S. Ilican, Y. Caglar, F. Yakuphanoglu, J. Mater. Sci. Mater. Electron. in press (2008).
[11] X. Peng, H. Zang, Z. Wang, J. Xu, Y. Wang, J. Luminescence **128** 328 (2008).
[12] G. Machado, D.N. Guerra, D. Leinen, J.R. Ramos-Barrado, R.E. Marotti, E.A. Dalchiele, Thin Solid Films **490** 124 (2005).
[13] S. Ilican, M. Caglar, Y. Caglar, Materials Science-Poland, **25** 709(2007).
[14] Y. Caglar, S. Ilican, M. Caglar, F. Yakuphanoglu, Spectrochimica Acta Part A **67** 1113 (2007).
[15] M.A. Lucio-Lopez, A. Maldonado, R. Castanedo-Perez, G. Torres-Delgado, M. de la L. Olvera, Sol. Energ. Mater. Solar Cells **90** 2362 (2006).
[16] E.J. Luna-Arredondo, A. Maldonado, R. Asomoza, D.R. Acosta, M.A. Melendez-Lira, M. de la L. Olvera, Thin Solid Films **490** 132 (2005).
[17] B. Wang, M.J. Callahan, Chunchuan Xu, L.O. Bouthillette, N.C. Giles, D.F. Bliss, J. Cryst. Growth **304** 73 (2007).
[18] M.A. Lucio-Lopez, M.A. Luna-Arias, A. Maldonado, M. de la L. Olvera, D.R. Acosta, Sol. Energ. Mater. Solar Cells **90** 733 (2006).
[19] J. Wienke, A.S. Booij, Thin Solid Films in press (2007).
[20] F. Yakuphanoglu, S. Ilican, M. Caglar, Y. Caglar, J. Optoelectron. Adv. Mater. **9**(7), 2180 (2007).
[21] Y. Caglar, M. Zor, N. Caglar, S. Ilican, J. Optoelectron. Adv. Mater. **8**(5), 1867 (2006).
[22] S. Ilican, Y Caglar, M. Caglar, J. Optoelectron. Adv. Mater. **10**(10), 2578 (2008).
[23] B.D. Cullity, S.R. Stock, Elements of X-Ray Diffraction, Prentice Hall, 2001, 3rd ed.
[24] C.S. Barret, T.B. Massalski, Structure of Metals, Pergamon Press, Oxford, (1980)
[25] J. I. Pankove, Optical Processes in Semiconductors, Prentice-Hall Inc., Englewoord Cliffs, NJ, (1971).
[26] F. Urbach, Phys Rev. **92** 1324 (1953).
[27] A. K. Wolaton, T.S. Moss, Proc. Roy. Soc. B. **81** 5091*(*1963).
[28] N. A. Subrahamanyam, A textbook of Optics, 9th ed;Brj Laboratory, Delhi, India, (1977).
[29] T.S. Moss, G.J. Burrell, B. Ellis, Semiconductor Opto-Electronics, Wiley, New York, (1973).
[30] L. J. Van der Pauw, Philips Res. Repts. **13** 1 (1958).
[31] R. G. Gordon, Mater. Res. Soc. Symp. **426**, 419 (1996).

*Corresponding author: silican@anadolu.edu.tr